ACS Photonics

Letter

pubs.acs.org/journal/apchd5

Shape-Controlled Assembly of Nanowires for Photonic Elements

You-Shin No,[†,‡] Lin Xu,[*,‡] Max N. Mankin,[‡] and Hong-Gyu Park[*,†]

[†]Department of Physics, Korea University, Seoul 136-701, Republic of Korea

[‡]Department of Chemistry and Chemical Biology, Harvard University, Cambridge, Massachusetts 02138, United States

ABSTRACT: We fabricated a single U-shaped nanowire (NW) and tangent-coupled straight and U-shaped NWs using a novel technique of shape-controlled deterministic assembly of NWs with nanoscale controllability. To examine the optical properties of these structures, we calculated the transmitted and crossover optical powers of the fundamental guided mode in both the single and coupled CdS NWs by varying the key structural parameters such as the radius of curvature of the U-shaped head and the gap between the NWs. In addition, we experimentally studied active waveguiding in the assembled CdS NWs, which exhibited light coupling to the waveguide mode and direct transmission in the single U-shaped NW. Furthermore, the crossover coupling was measured for the tangent-coupled straight and U-shaped CdS NWs with a gap width of 70 nm. The shape-controlled deterministic assembly technique can open up a new opportunity to demonstrate subwavelength-scale photonic waveguides and couplers in compact nanophotonic integrated circuits.

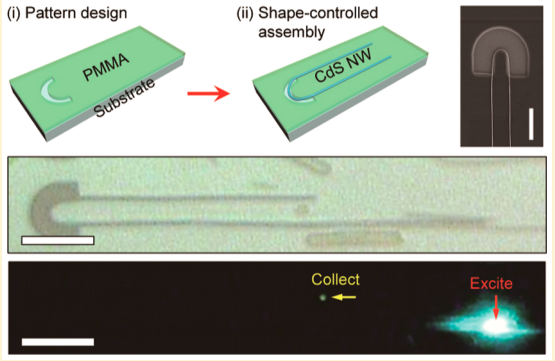

KEYWORDS: *nanowire assembly, optical waveguides, optical couplers, cadmium sulfide nanowires, FDTD simulation method*

High-index semiconductor nanowires (NWs) are promising building blocks for on-chip integration of nanophotonic devices, because they can strongly confine electromagnetic waves in a subwavelength-scale volume and support guided optical modes.[1−6] These NWs have been utilized as key photonic elements in single- and multicolor nanoscale light-emitting diodes (LEDs),[7,8] polarization-sensitive photodetectors,[9] electrically and optically driven low-threshold lasers,[10−14] active photonic waveguides,[15,16] electro-optic modulators,[17] and all-optical switches.[18] However, despite the successful demonstration of these devices in a single NW level, it has been a challenge to precisely control the position, geometry, and alignment of individual NWs for the seamless integration in a compact photonic circuit.[19−21] Recent advances in controlled nanoscale assembly techniques have enabled the development of a variety of bottom-up nanodevices that cannot be realized using conventional postgrowth assembly of NWs.[22,23] For example, a nanocombing assembly method has allowed simultaneous control of position and alignment of NWs and facilitated the large-scale fabrication of hierarchical arrays of single NW devices.[22] More recently, a wafer-scale, shape-controlled deterministic assembly method has demonstrated a high yield (∼90%) of individually addressable U-shaped three-dimensional (3D) NW field-effect transistor arrays.[23] These successful demonstrations of NW assembly have motivated researchers to explore potential optical and biological applications. In particular, photonic elements such as waveguides and couplers can be deterministically formed by a well-controlled assembly of semiconductor NWs at targeted locations on a receiving substrate. In this work, we demonstrate shape-controlled and deterministically configured CdS NW active photonic elements using such a novel assembly technique. Our numerical simulations show that efficient light propagation, controllable transmission, and crossover coupling are feasible in single U-shaped NW waveguides and coupled straight and U-shaped NW photonic couplers. In addition, we performed simple proof-of-concept active waveguiding and light coupling experiments using the fabricated tangent-coupled straight and U-shaped CdS NWs.

Figure 1a schematically illustrates deterministic and shape-controlled assembly of NWs. The fabrication steps involve (i) patterning of trenches with predesigned shape in a resist layer surface on the target substrate and (ii) shear-transferring of the synthesized NWs from the growth substrate to the target substrate. The patterned trenches serve as anchoring windows, while the synthesized NWs are transferred by the linear translation with a fixed normal load and specific orientation.[23] The radius of curvature of the assembled NW depends on the contact pressure during the shear transfer and the NW diameter.[23] The representative scanning electron microscopy (SEM) image in Figure 1a shows a single CdS NW with a diameter of ∼150 nm, which was successfully assembled using a designed U-shaped poly(methyl methacrylate) (PMMA) trench with an inner radius of curvature of 2 μm on a SiO_2 target substrate. We then performed finite-difference time-domain (FDTD) simulations to investigate the optical properties of the fabricated CdS NW as a photonic waveguide. First, we calculated the dispersion curves of guided optical modes in an infinitely long CdS NW with a circular cross section and a

Received: October 10, 2016
Published: November 9, 2016

DOI: 10.1021/acsphotonics.6b00775
ACS Photonics 2016, 3, 2285−2290

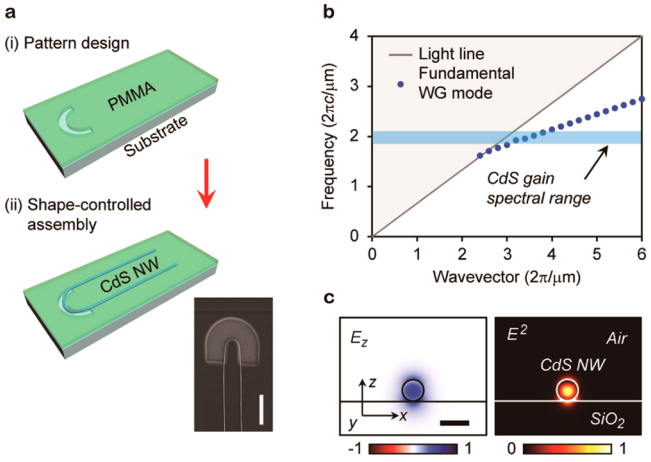

Figure 1. Shape-controlled deterministic assembly of a NW photonic waveguide and optical properties of the fundamental waveguide mode. (a) Schematics of key assembly steps: (i) patterning of a trench with a predesigned shape (U-shape) in a resist surface layer on the target substrate and (ii) shear-transferring of NWs from the growth substrate to the target substrate. Inset: SEM image of a typical assembled CdS NW. The scale bar is 5 μm. (b) Calculated dispersion curve of the fundamental waveguide mode in an infinitely long CdS NW photonic waveguide with a diameter of 150 nm (dark blue dots). The blue and gray lines indicate the gain spectral range of the CdS and the light line, respectively. The normalized frequency and wavevector are in the units of $2\pi c/\mu$m and $2\pi/\mu$m, respectively. (c) Electric field (E_z) and intensity (E^2) profiles of the fundamental waveguide mode in the NW on a SiO_2 substrate. The scale bar is 200 nm.

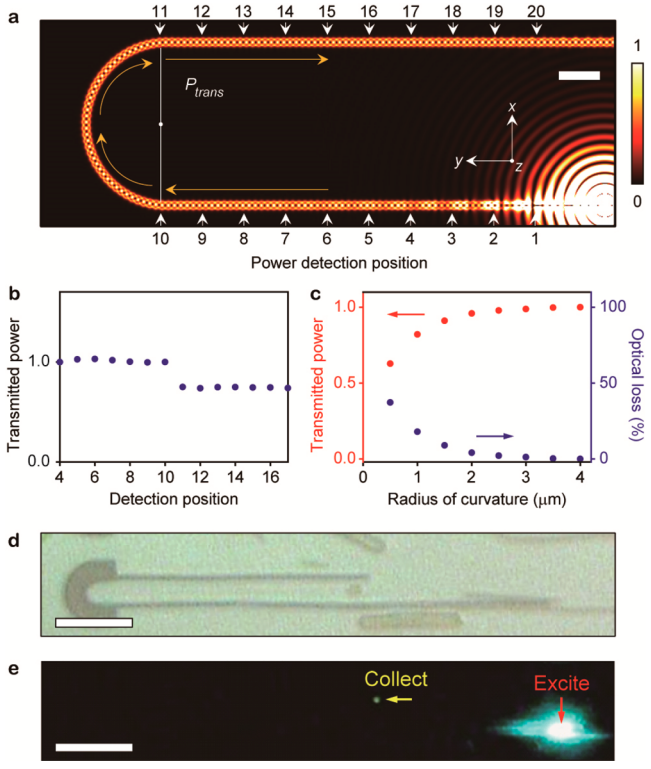

Figure 2. Simulation and measurement of light propagation in single U-shaped NW photonic waveguides. (a) Calculated electric field intensity distribution of the propagating fundamental waveguide mode in a single U-shaped NW photonic waveguide on the SiO_2 substrate. The radius of curvature of the U-shaped head and the length of one straight arm of the waveguide were 2 and 11 μm, respectively. The diameter of the NW was 150 nm. Numbers (1−20) with white arrows indicate the measurement locations of the transmitted power along the NW waveguide. Adjacent locations are 1 μm apart. The scale bar is 1 μm. (b) Calculated transmitted power (dark blue dots) as a function of the measurement location along the NW waveguide. The transmitted power was normalized by the transmitted power at location 10. (c) Calculated transmitted power (red dots) and optical loss (dark blue dots) as a function of the radius of curvature of the U-shaped NW. (d) Optical microscopy image of the fabricated U-shaped CdS NW. The NW diameter is ~150 nm. The U-shaped PMMA trench was defined on the SiO_2 substrate. (e) Measurement of active waveguiding in the U-shaped NW in (d). The red and yellow arrows indicate the optical excitation and the collection of waveguided light, respectively. The scale bars are 8 μm in (d) and (e).

diameter of 150 nm on a SiO_2 substrate (Figure 1b). In the simulation, periodic boundary conditions were used in the direction parallel to the NW axis, and perfectly matched layers (PMLs) were introduced to the other boundaries. The refractive indices of CdS and SiO_2 were set to 2.7 and 1.5, respectively.[24,25] The NW supports only the fundamental waveguide mode (dark blue dots) within the gain spectral range of CdS (light blue line) (Figure 1b). The electric field and intensity distributions show the tight confinement of fields at the center of NWs (Figure 1c).

Next, we performed a 3D FDTD simulation of light propagation in a single U-shaped NW photonic waveguide (Figure 2a). The symmetric U-shaped NW consisted of one U-shaped head with a radius of curvature (R) of 2 μm and two 11-μm-long straight arms. Other structural and material parameters, including boundary conditions, NW cross section, and refractive indices, were the same as those for the data in Figure 1b. To simulate optical excitation and light propagation, an excitation dipole source with a wavelength of 515 nm was introduced at one end of the U-shaped NW arm. The calculated electric field intensity profile in Figure 2a shows that the emitted light is coupled to the fundamental waveguide mode, which propagates through one arm of the waveguide, makes a U-turn, and propagates back toward the other end of the NW arm. In Figure 2b, we calculated the transmitted optical power at different locations along the NW (white arrows in Figure 2a). The distance between two adjacent locations was 1 μm, and location 1 was 2 μm away from the end of the NW arm. The transmitted power was calculated by integrating the total flux of the Poynting vectors passing through the surface including the NW cross section. Then, the calculated transmitted power was normalized with respect to the transmitted power at location 10, where the U-shaped head started. A negligible variation in the transmitted power was observed in the straight arms, whereas a noticeable power loss of ~4% was observed between locations 10 and 11 (Figure 2b). This optical loss originated from evanescent fields along the bent U-shaped head.[26−28] To further investigate the optical properties, we systematically varied the R value of the U-shaped head from 0.5 μm to 4 μm with a step size of 0.5 μm (Figure 2c), calculated the normalized transmitted power (red dots), and subsequently estimated the optical loss (dark blue dots) of the fundamental waveguide mode. For R > 2 μm, the optical loss was negligible and the power was efficiently transmitted through the U-shaped head. However, for R comparable to the size of the wavelength, electric fields of the waveguide mode leaked out from the abruptly bent U-shaped head in the waveguide, incurring significant optical loss (e.g., 37.2% for R = 0.5 μm).[27,28]

DOI: 10.1021/acsphotonics.6b00775
ACS Photonics 2016, 3, 2285−2290

To experimentally demonstrate the propagation of light in single U-shaped NW photonic waveguides, we fabricated U-shaped trenches with an inner R of 2 μm in a PMMA surface layer on a SiO_2 substrate and assembled CdS NWs with diameters of ~150 nm (Figure 2d). Then, a continuous-wave diode laser with a wavelength of 405 nm was used to excite one end of the straight arms of the NWs. The incident power of the pump laser was ~40 μW, and the laser spot size was ~1 μm in diameter. A wide-field photoluminescence image was collected through a 20× microscope objective lens with numerical aperture (NA) of 0.5 (Figure 2e). We observed a strong photoluminescence emission at one end of the U-shaped NW by optical pumping (red arrow; excitation) and a small but clear light spot at the other end (yellow arrow; collection). The measurement clearly shows that the photoluminescence is coupled to a waveguide mode propagating along the NW and is scattered out at the end of the other arm of the NW, which qualitatively agrees with the simulation results.

We further explored the ability of our shape-controlled and deterministic NW assembly technique by fabricating more complex coupled NW structures with nanoscale controllability. Figure 3a illustrates simple two-step assembly procedures for fabricating tangent-coupled straight and U-shaped NWs. First, electron-beam lithography was used for defining simple rectangular trenches on a target substrate to anchor and align a straight NW (Figure 3a, (i)). Next, another round of lithography was performed to fixate the straight NW and define a U-shaped trench with a designed R and a controlled gap width (g) between the NW and the trench pattern. Shear-transferring the NW growth substrate with the orientation perpendicular to that of the straight NW registered the second NW at the U-shaped trench and aligned the two straight arms of the U-shaped NW (Figure 3a, (ii)). Finally, the assembled NW was fixated by additional lithography, and the residual resist was removed (Figure 3a, (iii)). This completed the two-step assembly of the tangent-coupled straight and U-shaped NW structures with a controlled gap width. We conducted experiments to examine the viability of our assembly technique, using Si NWs with uniform diameters of ~80 nm. The SEM image in Figure 3b (left panel) shows a straight NW tightly coupled to the tip of the U-shaped NW's head. Cross-linked PMMA patches were used to fixate the two straight arms of the U-shaped NW. Figure 3b (right panel) shows the magnified SEM image of the central coupling region; the straight and U-shaped NWs are separated by a ~70-nm-wide gap, which is comparable to the NW diameter. In addition, we successfully fabricated the same coupled structure but with a ~140-nm-wide gap (Figure 3c). This result shows that the spatial accuracy of the shear transfer is good enough to precisely control the gap width of the tangent-coupled NW configuration. Also, our assembly technique can be extended to the assembly of various one-dimensional nanomaterials on single-target substrates. Therefore, one can efficiently utilize the technique and fabricate more complex structures consisting of two different materials, which have been challenging using conventional top-down nanofabrication technology.

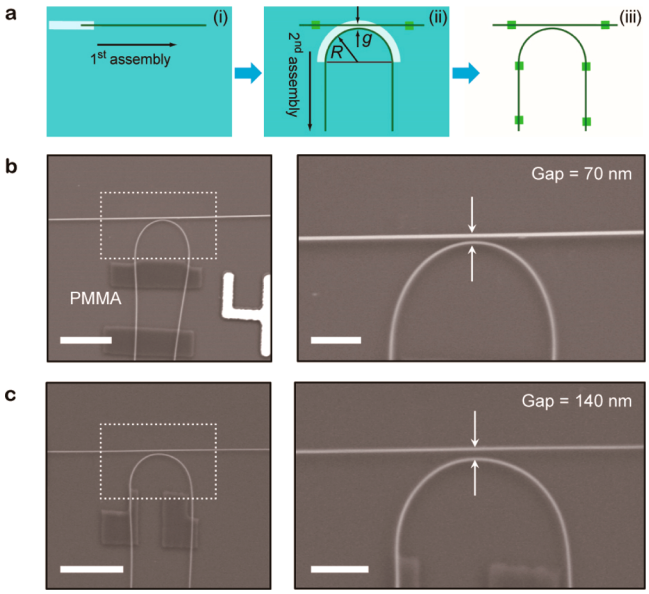

Figure 3. Two-step deterministic assembly of NWs for a coupled NW structure with nanoscale controllability. (a) Schematics of the two-step assembly process for tangent-coupled straight and U-shaped NWs: (i) a straight NW (first assembly) is transferred in a surface resist layer on a target substrate, (ii) a U-shaped trench is defined and the second NW is transferred (second assembly), and (iii) the U-shaped NW is fixated and the residual resist is removed. (b, c) Low (left panel) and high (right panel) magnification SEM images of shape-controlled and deterministically assembled straight and U-shaped Si NWs with controlled gap widths of (b) 70 nm and (c) 140 nm, respectively. The diameters of the NWs were ~80 nm. Left panel: Cross-linked PMMA patches were used to fixate the assembled NWs. The scale bars are 3 μm. Right panel: Magnified SEM images of the white dotted boxes in the left panels. The scale bars are 1 μm.

To explore the optical properties of tangent-coupled straight and U-shaped CdS NWs, we performed systematic 3D FDTD simulations. In these simulations, the length of one arm was set to 10 μm, R of the U-shaped NW was set to 4 μm, and the length of the straight NW was set to 22 μm. The gap width between the straight and U-shaped NWs was set to 70 nm. The other structural and material parameters were the same as the ones used for the data in Figure 2. Two different locations of the dipole excitation with a wavelength of 515 nm at one end of the U-shaped (Figure 4a) and the straight (Figure 4b) NWs were considered. We then calculated the transmitted power of the fundamental waveguide mode in the straight and U-shaped NWs, before (P_0) and after (P_1 and P_2) the central coupling region. In Figure 4a, P_0 and P_1 are the optical powers at the start and end positions of the U-shaped head, respectively, whereas P_2 is the transmitted power in the straight NW, 6 μm away from the center of coupling region. Similarly, in Figure 4b, P_0 and P_1 were calculated for the straight NW, 1 and 6 μm away from the center of the straight NW to the right and left directions, respectively, whereas P_2 was calculated at the end of the U-shaped head. In both cases, P_1 and P_2 were normalized with respect to P_0, to calculate transmission (P_{trans}) and crossover coupling (P_{cross}) between the two NWs. Figure 4c and d show the calculated P_{trans} (left y-axis) and P_{cross} (right y-axis) as a function of gap width, for the coupling structures in Figure 4a and b, respectively. For the gap width of 70 nm in the structure in Figure 4a (Figure 4b), P_{trans} and P_{cross} were ~57% and ~41% (~58% and ~41%), respectively, and the estimated optical loss during the coupling was ~2% (1%). Such a comparable transmission and crossover coupling with a negligibly small optical loss in each excitation scheme is attributed to the large R and small gap width: efficient transmission and crossover coupling occur before the propagating light is lost in the form of evanescent fields in

DOI: 10.1021/acsphotonics.6b00775
ACS Photonics 2016, 3, 2285−2290

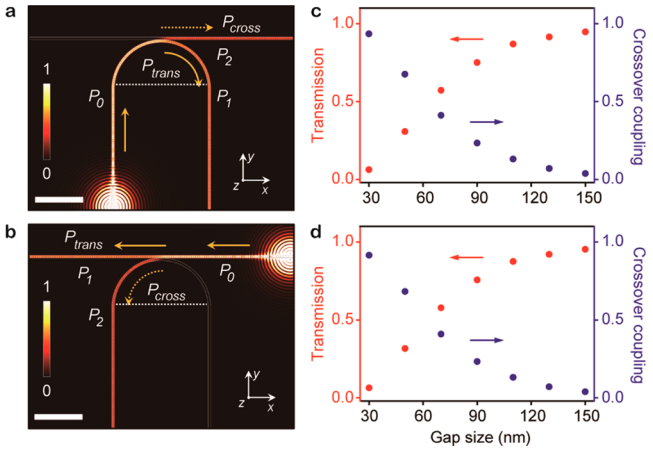

Figure 4. Simulations of light propagation in tangent-coupled straight and U-shaped CdS NW photonic couplers. (a, b) Calculated electric field intensity distributions with the excitations at one end of U-shaped (a) and straight (b) NWs. The diameters of the NWs and the excitation wavelength were 150 and 515 nm, respectively. The gap width between the straight and U-shaped NWs was 70 nm. The scale bars are 5 μm. The transmitted power in one NW before and after the central coupling region is P_0 and P_1, respectively, and the coupled power in the other NW is P_2. The transmission and crossover coupling are defined as $P_{trans} = P_1/P_0$ and $P_{cross} = P_2/P_0$, respectively. (c, d) Calculated transmission (red dots, left axis) and crossover coupling (dark blue dots, right axis) vs the gap width, in the coupling structures in panel a (c) and panel b (d). The gap width varied from 30 to 150 nm, in steps of 20 nm.

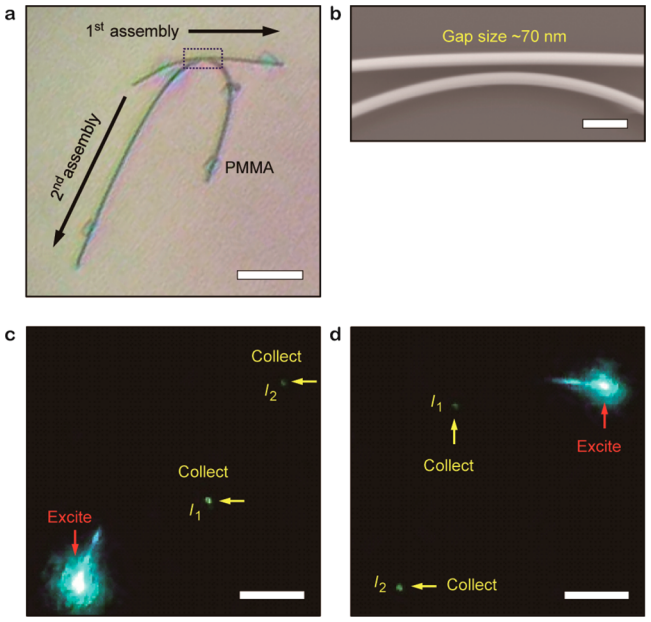

Figure 5. Deterministically assembled coupled CdS NWs photonic coupler. (a) The optical microscopy image shows the photonic coupler consisting of the straight and U-shaped CdS NWs on the SiO_2 substrate. The U-shaped NW was slightly rotated with respect to the axis perpendicular to the straight NW in the central coupling region. PMMA patches fixated the NWs. The scale bar is 10 μm. (b) Magnified SEM image of the coupling region (the black dotted box in (a)), showing a gap of ~70 nm between the straight and U-shaped NWs. The scale bar is 400 nm. (c, d) Collected photoluminescence images of light excitation (red arrows), direct transmission (yellow arrows, I_1), and crossover coupling (yellow arrows, I_2) in the tangent-coupled straight and U-shaped CdS NWs. The excitation positions are at one end of the U-shaped (c) and straight (d) NWs. The scale bars are 10 μm.

the coupling region. In addition, such a small loss likely arises owing to the mode coupling between the two same-diameter NWs.[29]

Next, for each excitation scheme, the gap width was varied from 30 to 150 nm with a step size of 20 nm (Figure 4c and d). The overall trends were very similar in both cases. For example, when the gap is smaller than 70 nm, P_{cross} became dominant. For such narrow gaps, the propagating waveguide mode in an excited NW experiences an abrupt and strong refractive index variation near the center of the coupling region. As a result, a small variation in the wavevector of the original waveguide mode and preferential coupling to the waveguide mode in the other NW occur (e.g., ~93% of crossover coupling for g = 30 nm).[28,29] However, for gaps wider than 70 nm, the evanescent fields decay rapidly in the surroundings before light coupling to the other NW occurs, significantly reducing the crossover coupling strength (e.g., ~4% of crossover coupling for g = 150 nm). The estimated optical loss remained at ~2% or less for all cases owing to the efficient crossover coupling (for g < 70 nm) and large R of the U-shaped head (for g > 70 nm).

Finally, we performed a proof-of-concept optical experiment and demonstrated the light propagation and crossover coupling between the tangent-coupled straight and U-shaped NWs. The two-step assembly technique schematically shown in Figure 3 was used for fabricating a coupled structure consisting of two CdS NWs, each with a diameter of ~150 nm. In Figure 5a, the optical microscopy image shows that the U-shaped NW was successfully assembled but slightly rotated with respect to the axis perpendicular to the straight NW. A magnified SEM image of the coupling region (Figure 5b; indicated by a dotted box in Figure 5a) shows that a small gap width of ~70 nm was well-defined between the two NWs. Then, we performed optical experiments for active waveguiding and light coupling. First, one end of the U-shaped NW was excited by a 405-nm-wavelength laser diode (the red arrow in Figure 5c), similar to the situation in Figure 2e. Emission of light from the other end of the U-shaped NW (yellow arrow, I_1) and one end of the straight NW (yellow arrow, I_2) was clearly observed. The waveguided light through the U-shaped NW was observed at I_1 (direct transmission), whereas the coupled light from the U-shaped NW to the straight NW was observed at I_2 (crossover coupling). The measured emission intensity ratio, I_1/I_2, was estimated as ~2.7. Next, by optical pumping of one end of the straight NW (the red arrow in Figure 5d), emission of the waveguided light in the straight NW (direct transmission, I_1) and the coupled light to the U-shaped NW (crossover coupling, I_2) was observed. In this case, the measured emission intensity ratio, I_2/I_1, was ~2.0. These proof-of-concept experiments qualitatively agree with the simulation results in Figure 4, although the measured output intensity ratio I_1/I_2 and the calculated power ratio P_{trans}/P_{cross} are quantitatively different. In fact, a slight variation in the diameter of our synthesized CdS NWs, i.e., different NW diameters at the excitation and collection locations, can induce light intensity variation when the guided light is re-emitted or scattered out. In addition, other assembly parameters, such as rotational tuning of the gap between the NWs, can adjust the intensity ratio between the direct transmission and crossover coupling.

In conclusion, we have utilized the novel technique of shape-controlled deterministic assembly of NWs and fabricated

DOI: 10.1021/acsphotonics.6b00775
ACS Photonics 2016, 3, 2285−2290

tangent-coupled straight and U-shaped NW structures with nanoscale controllability. The optical properties of the fundamental waveguide mode in single and coupled CdS NWs (for photonic waveguides and couplers) were theoretically investigated using 3D FDTD simulations. P_{trans} and P_{cross} were systematically calculated, by varying the structural parameters such as R of the U-shaped head and g between the NWs. For example, P_{trans} and P_{cross} were calculated to be ~58% and ~41% for g = 70 nm of the coupled NW structures. Active waveguiding and direct transmission were experimentally observed in the single U-shaped CdS NW with a diameter of 150 nm and R of 2 μm. In addition, crossover coupling was successfully demonstrated in the tangent-coupled straight and U-shaped CdS NWs with g = 70 nm. We believe that the described shape-controlled assembly technique will become important for designing and studying nanoscale integrated photonic circuits and for exploring novel promising optical applications.

METHODS

Synthesis of CdS NWs. Cadmium sulfide (CdS) NWs were synthesized using a gold (Au) nanoparticle-catalyzed vapor−liquid−solid (VLS) process. The Au nanoparticles with diameters of 150 nm (15712, Ted Pella) were dispersed on the SiO_2/Si growth substrates (600 nm thermal SiO_2). In our chemical vapor deposition (CVD) system, CdS powder (99.999%, Alfa Aesar) was evaporated in the high-temperature zone and NWs were synthesized on the substrates in the downstream lower temperature zone. The CdS evaporation temperature was 675 °C, growth zone temperature was 600 °C, H_2 carrier gas flow rate was 20 sccm, total pressure was 2.8 Torr, and growth time was 60 min.

Fabrication of U-Shaped NW Structures. The PMMA U-shaped trenches were defined on the SiO_2/Si target substrates using electron-beam lithography. The target substrate was then mounted onto a micromanipulator-controlled moveable stage and covered with mineral oil (330760, Sigma-Aldrich). The CdS NW growth substrate was brought into contact with the target substrate with a contact pressure of 4.8 N/cm^2. The target substrate was linearly translated at a constant velocity of ~5 mm/min with respect to the fixed NW growth substrate to generate U-shaped NW structures. The target substrate was finally rinsed with octane (98%, Sigma-Aldrich) to remove the lubricant. For the tangent-coupled straight and U-shaped NW configuration, the two-step assembly process was used (Figure 3). The second shear transfer was performed along the direction perpendicular to that of the registered straight NW by the first transfer.

Optical Measurement. A continuous-wave laser diode with a wavelength of 405 nm (LRD-0405, LaserGlow Technologies) was used to excite NWs. Wide-field photoluminescence images were collected using a 20× microscope objective lens with NA of 0.5. The incident power of the pump laser was ~40 μW, and the laser spot size was ~1 μm in diameter.

FDTD Simulations. In the FDTD simulations, the refractive indices of CdS and SiO_2 were 2.7 and 1.5, respectively. To calculate the dispersion curve in an infinitely long single CdS NW (Figure 1b), a periodic boundary condition was used along the long axis of the NW, and perfectly matched layers were introduced at the other boundaries. The calculation domain size was 1.00 × 0.80 μm^2 and the spatial resolution was 5 nm. Transmitted powers and coupling efficiencies were calculated using the 3D FDTD method with a spatial resolution of 20 nm (Figures 2 and 4). The calculation domain sizes were 9.00 × 15.50 × 0.75 μm^3 and 22.00 × 16.80 × 0.75 μm^3 in Figures 2 and 4, respectively.

AUTHOR INFORMATION

Corresponding Authors

*E-mail: xulin678@gmail.com.
*E-mail: hgpark@korea.ac.kr.

ORCID

Hong-Gyu Park: 0000-0002-6375-0314

Notes

The authors declare no competing financial interest.

ACKNOWLEDGMENTS

We thank Prof. Charles M. Lieber for helpful discussions and offering fabrication and measurement facilities. H.-G.P. acknowledges support by the National Research Foundation of Korea (NRF) grant funded by the Korean government (MSIP) (No. 2009-0081565). Y.-S.N. acknowledges support by a Korea University Grant.

REFERENCES

(1) Huang, Y.; Duan, X.; Lieber, C. M. Nanowires for Integrated Multicolor Nanophotonics. *Small* **2005**, *1*, 142−147.
(2) Agarwal, R.; Lieber, C. M. Semiconductor nanowires: optics and optoelectronics. *Appl. Phys. A: Mater. Sci. Process.* **2006**, *85*, 209−215.
(3) Yan, R.; Gargas, D.; Yang, P. D. Nanowire photonics. *Nat. Photonics* **2009**, *3*, 569−576.
(4) Cao, L.; White, J. S.; Park, J.-S.; Schuller, J. A.; Clemens, B. M.; Brongersma, M. L. Engineering light absorption in semiconductor nanowire devices. *Nat. Mater.* **2009**, *8*, 643−647.
(5) Kim, S.-K.; Day, R. W.; Cahoon, J. F.; Kempa, T. J.; Song, K.-D.; Park, H.-G.; Lieber, C. M. Tuning Light Absorption in Core/Shell Silicon Nanowire Photovoltaic Devices through Morphological Design. *Nano Lett.* **2012**, *12*, 4971−4976.
(6) Day, R. W.; Mankin, M. N.; Gao, R.; No, Y.-S.; Kim, S.-K.; Bell, D. C.; Park, H.-G.; Lieber, C. M. Plateau−Rayleigh crystal growth of periodic shells on one-dimensional substrates. *Nat. Nanotechnol.* **2015**, *10*, 345−352.
(7) Qian, F.; Gradecak, S.; Li, Y.; Wen, C.-Y.; Lieber, C. M. Core/Multishell Nanowire Heterostructures as Multicolor, High-Efficiency Light-Emitting Diodes. *Nano Lett.* **2005**, *5*, 2287−2291.
(8) No, Y.-S.; Choi, J.-H.; Ee, H.-S.; Hwang, M.-S.; Jeong, K.-Y.; Lee, E.-K.; Seo, M.-K.; Kwon, S.-H.; Park, H.-G. A Double-Strip Plasmonic Waveguide Coupled to an Electrically Driven Nanowire LED. *Nano Lett.* **2013**, *13*, 772−776.
(9) Wang, J.; Gudiksen, M. S.; Duan, X.; Cui, Y.; Lieber, C. M. Highly Polarized Photoluminescence and Photodetection from Single Indium Phosphide Nanowires. *Science* **2001**, *293*, 1455−1457.
(10) Agarwal, R.; Barrelet, C. J.; Lieber, C. M. Lasing in Single Cadmium Sulfide Nanowire Optical Cavities. *Nano Lett.* **2005**, *5*, 917−920.
(11) Gradecak, S.; Qian, F.; Li, Y.; Park, H.-G.; Lieber, C. M. GaN nanowire lasers with low lasing thresholds. *Appl. Phys. Lett.* **2005**, *87*, 173111.
(12) Qian, F.; Li, Y.; Gradecak, S.; Park, H.-G.; Dong, Y.; Ding, Y.; Wang, Z. L.; Lieber, C. M. Multi-quantum-well nanowire heterostructures for wavelength-controlled lasers. *Nat. Mater.* **2008**, *7*, 701−706.
(13) Oulton, R. F.; Sorger, V. J.; Zentgraf, T.; Ma, R.-M.; Gladden, C.; Dai, L.; Bartal, G.; Zhang, X. Plasmon lasers at deep subwavelength scale. *Nature* **2009**, *461*, 629−632.
(14) Duan, X.; Huang, Y.; Agarwal, R.; Lieber, C. M. Single-nanowire electrically driven lasers. *Nature* **2003**, *421*, 241−245.

DOI: 10.1021/acsphotonics.6b00775
ACS Photonics 2016, 3, 2285−2290

(15) Barrelet, C. J.; Greytak, A. B.; Lieber, C. M. Nanowire Photonic Circuit Elements. *Nano Lett.* **2004**, *4*, 1981−1985.
(16) Sirbuly, D. J.; Law, M.; Pauzauskie, P.; Yan, H.; Maslov, A. V.; Knutsen, K.; Ning, C.-Z.; Saykally, R. J.; Yang, P. D. Optical routing and sensing with nanowire assemblies. *Proc. Natl. Acad. Sci. U. S. A.* **2005**, *102*, 7800−7805.
(17) Greytak, A. B.; Barrelet, C. J.; Li, Y.; Lieber, C. M. Semiconductor nanowire laser and nanowire waveguide electro-optic modulators. *Appl. Phys. Lett.* **2005**, *87*, 151103.
(18) Piccione, B.; Cho, C.-H.; Vugt, L. K. V.; Agarwal, R. All-optical active switching in individual semiconductor nanowires. *Nat. Nanotechnol.* **2012**, *7*, 640−645.
(19) Park, H.-G.; Barrelet, C. J.; Wu, Y.; Tian, B. Z.; Quian, F.; Lieber, C. M. A wavelength-selective photonic-crystal waveguide coupled to a nanowire light source. *Nat. Photonics* **2008**, *2*, 622−626.
(20) Wang, M. C. P.; Gates, B. D. Directed assembly of nanowires. *Mater. Today* **2009**, *12*, 34−43.
(21) Lu, W.; Lieber, C. M. Nanoelectronics from the bottom up. *Nat. Mater.* **2007**, *6*, 841−850.
(22) Yao, J.; Yan, H.; Lieber, C. M. A nanoscale combing technique for the large-scale assembly of highly aligned nanowires. *Nat. Nanotechnol.* **2013**, *8*, 329−335.
(23) Zhao, Y.; Yao, J.; Xu, L.; Mankin, M. N.; Zhu, Y.; Wu, H.; Mai, L.; Zhang, Q.; Lieber, C. M. Shape-Controlled Deterministic Assembly of Nanowires. *Nano Lett.* **2016**, *16*, 2644−2650.
(24) Barrelet, C. J.; Wu, Y.; Bell, D. C.; Lieber, C. M. Synthesis of CdS and ZnS Nanowires Using Single-Source Molecular Precursors. *J. Am. Chem. Soc.* **2003**, *125*, 11498−11499.
(25) Ninomiya, S.; Adachi, S. Optical properties of wurtzite CdS. *J. Appl. Phys.* **1995**, *78*, 1183−1190.
(26) Sakai, J.-I.; Kimura, T. Bending loss of propagation modes in arbitrary-index profile optical fibers. *Appl. Opt.* **1978**, *17*, 1499−1506.
(27) Yu, H.; Wang, S.; Fu, J.; Qiu, M.; Li, Y.; Gu, F.; Tong, L. Modeling bending losses of optical nanofibers or nanowires. *Appl. Opt.* **2009**, *48*, 4365−4369.
(28) Yariv, A.; Yeh, P. *Photonics: Optical Electronics in Modern Communications*; Oxford: New York, 2007.
(29) Latawiec, P.; Burek, M. J.; Venkataraman, V.; Loncar, M. Waveguide-loaded silica fibers for coupling to high-index microresonators. *Appl. Phys. Lett.* **2016**, *108*, 031103.

DOI: 10.1021/acsphotonics.6b00775
ACS Photonics 2016, 3, 2285−2290